Sulfur-containing histidine compounds inhibit γ-glutamyl transpeptidase activity in human cancer cells

Received for publication, May 10, 2019, and in revised form, July 4, 2019 Published, Papers in Press, August 2, 2019, DOI 10.1074/jbc.RA119.009304

Mariarita Brancaccio[‡1,2], Maria Russo[§1], Mariorosario Masullo[¶], Anna Palumbo[‡], Gian Luigi Russo[‡§], and Immacolata Castellano[‡3]

From the [‡]Department of Biology and Evolution of Marine Organisms, Stazione Zoologica Anton Dohrn, 80121 Naples, Italy, [§]Institute of Food Sciences, National Research Council, 83100 Avellino, Italy, and [¶]Department of Movement Sciences and Wellbeing, University of Naples "Parthenope," 80133 Naples, Italy

Edited by F. Peter Guengerich

γ-Glutamyl transpeptidase (GGT) is an enzyme located on the surface of cellular membranes and involved in GSH metabolism and maintenance of redox homeostasis. High GGT expression on tumor cells is associated with increased cell proliferation and resistance against chemotherapy. GGT inhibitors evaluated so far in clinical trials are too toxic for human use. In this study, using enzyme kinetics analyses, we demonstrate that ovothiols, 5(*Nπ*)-methyl thiohistidines of marine origin, act as noncompetitive inhibitors of GGT, with an apparent K_i of 21 μM, when we fixed the concentrations of the donor substrate. We found that these compounds are more potent than the known GGT inhibitor 6-diazo-5-oxo-L-norleucine and are not toxic toward human embryonic cells. In particular, cellular process–specific fluorescence-based assays revealed that ovothiols induce a mixed cell-death phenotype of apoptosis and autophagy in GGT-overexpressing cell lines, including human liver cancer and chronic B leukemic cells. The findings of our study provide the basis for further development of 5-thiohistidines as therapeutics for GGT-positive tumors and highlight that GGT inhibition is involved in autophagy.

γ-Glutamyl transpeptidase (GGT)[4] is an enzyme (EC 2.3.2.2), localized on the outside of the cell surface, that catalyzes the hydrolysis of extracellular glutathione (GSH), thus providing the cell a source of cysteine for increased synthesis of intracellular GSH (1). In detail, GGT catalyzes the cleavage of γ-glutamyl compounds and the transfer of the γ-glutamyl group to an acceptor substrate by a ping–pong mechanism (2, 3). GSH, the most common physiological substrate of GGT, acts as the γ-glutamyl donor in the initial reaction of hydrolysis, and then cysteinyl-glycine is released and cleaved into cysteine and glycine by cell-surface dipeptidases. In the second reaction catalyzed by GGT (transpeptidation), the γ-glutamyl group is transferred from the γ-glutamyl-GGT complex to water to release glutamate or to a second substrate (the acceptor), usually consisting in amino acids or dipeptides. However, although the hydrolysis of GSH is the most accepted biological function for GGT, the transpeptidation reaction is far from being demonstrated to really occur in the cell (3). Several human tumors, including hepatocellular carcinoma and renal cell carcinoma, exhibit high levels of GGT activity, which enhances their resistance to chemotherapy due to GGT ability to recycle GSH (1, 4–7). Indeed, elevated GSH levels in tumors have been shown to contribute to chemo- and radiotherapy resistance and prevent the initiation of the apoptotic cascade in tumor cells (8, 9). When inhibiting GGT for as little as 2 h, the intracellular cysteine concentration in GGT-positive tumors is significantly reduced (10). In GGT-knockout mice, the absence of GGT in the renal proximal tubules results in the excretion of GSH in the urine (11). In these mice, GSH in the glomerular filtrate cannot be cleaved into its constituent amino acids for reabsorption. As a consequence, these mice grow slowly and finally die due to cysteine deficiency. Intense efforts are continuously devoted to identifying new inhibitors of GGT due to their therapeutic potential in the treatment of GGT-dependent pathologies such as some types of cancer, ischemia/reperfusion-induced renal injury, asthma, and liver fibrosis (7, 12–14).

The most-known compounds that inhibit GGT include glutamine analogues and other amino acidic derivatives such as acivicin, 6-diazo-5-oxo-L-norleucine (DON), azaserine (15, 16), sulfur derivatives of L-glutamic acid (17), and γ-(monophenyl) phosphonoglutamate analogues (18, 19). However, most of these compounds have proved to be toxic (20–22) due to their interference with essential pathways such as the glutamate recycling involved in neurotransmission. Among monophenyl phosphonoglutamate analogues, only the butanoic acid derivative GGsTop was found to be inactive on glutamine amidotransferase (23) and effective for the treatment of oral mucositis (24). In contrast, serine borate was found to be too weak as inhibitor (16, 25). Subsequently, a class of uncompetitive inhibitors, structurally different from and less toxic than the gluta-

This work was supported by Stazione Zoologica Anton Dohrn and the Institute of Food Sciences. The content of this study has been partially reported in the Italian Patent Application RBI15865-IT.
This article contains Figs. S1 and S2.
[1] Both authors contributed equally to this work.
[2] Supported by a Stazione Zoologica Anton Dohrn Naples Ph.D. fellowship.
[3] To whom correspondence should be addressed: Dept. of Biology and Evolution of Marine Organisms, Stazione Zoologica Anton Dohrn, Villa Comunale, 80121 Naples, Italy. Tel.: 39-081-5833206; E-mail: immacolata.castellano@szn.it.
[4] The abbreviations used are: GGT, γ-glutamyl transpeptidase; hGGT, human GGT; eqGGT, equine kidney GGT; GSH, glutathione; ovo, ovothiol A; DON, 6-diazo-5-oxo-L-norleucine; GpNA, γ-glutamyl-*para*-nitroanilide; GlyGly, glycyl-glycine; erg, ergothioneine; LC3, microtubule-associated protein 1A/1B light chain 3; NT, non-treated; MA, 3-methyladenine; Baf-A1, bafilomycin; HEK, human embryonic kidney; Bis-Tris, 2-[bis(2-hydroxyethyl)amino]-2-(hydroxymethyl)propane-1,3-diol; AFC, amino-4-trifluoromethylcoumarin.

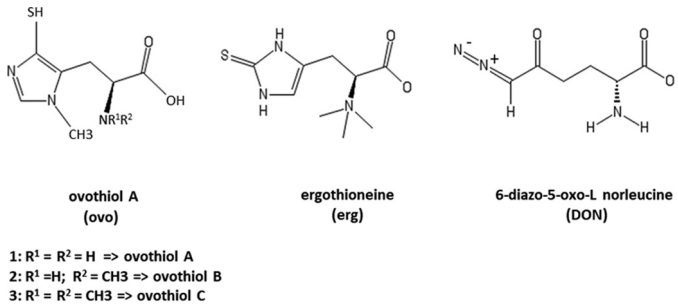

Figure 1. Sulfur-containing histidines and the GGT inhibitor DON. Chemical structures of ovo, erg, and DON.

mine analogs, were developed. These compounds do not interact with the γ-glutamyl–binding site, but they bind the acceptor site (26). However, no further *in vitro* and *in vivo* studies have confirmed their therapeutic potential.

In recent years, great attention has been focused on the marine environment as an unexplored reserve of new molecules with pharmacological potential. Among them, the class of thiohistidines, sulfur-containing natural products, has attracted researchers' attention for their redox properties (27, 28). In particular, 5-thiohistidines, mainly present in marine invertebrates, bacteria, and microalgae (29), occur either as free amino acids or as building blocks of complex thioalkaloids or iron-chelating pigments (29, 30). Briefly, 5(*Nπ*)-methyl thiohistidines, also named ovothiols, are known to play a key role in controlling the cellular redox balance for their ability to make a redox exchange with GSH (31–33). Ovothiol A (see Fig. 1 for the chemical structure) was isolated and characterized from the eggs of the sea urchin *Paracentrotus lividus* and from the ovary, eggs, and biological fluids of other marine invertebrates such as sea stars and cephalopods (29, 30). Moreover, ovothiol A was found in some human pathogens, marine worms (34, 35), and microalgae known for their high metabolic profile and potential in biotechnological applications (36, 37). The ovothiol derivatives B and C (Fig. 1), distinguished by one or two additional methyl groups at the α-amino group of 5-thiohistidine, were also discovered in the eggs of the spiny scallop *Chlamys hastata* and the sea urchins *Strongylocentrotus purpuratus* and *Sphaerechinus granularis* (29, 30). Recently, the enzymes responsible for ovothiol biosynthesis have been characterized (38, 39), and *in silico* analysis has revealed homologous genes in a wide range of genomes from Proteobacteria to Animalia (38). However, the finding that tetrapods' genomes lack the genes responsible for ovothiol biosynthesis (40) led to the investigation of their biological activities in mammalian models (14, 41, 42). In particular, we have recently demonstrated that ovothiol A induces autophagy in a human liver carcinoma cell line, HepG2 (41), and exhibits anti-inflammatory activity, when administered in its disulfide form, in an *in vivo* model of liver fibrosis (14). Overall, these studies prompted the total chemical synthesis of these compounds (43, 44), leading to the recently published synthetic protocol that starts from the natural precursor L-histidine (45). Here, we report for the first time the biochemical characterization of 5-thiohistidines as a novel class of GGT inhibitors to be potentially employed in the treatment of GGT-positive diseases.

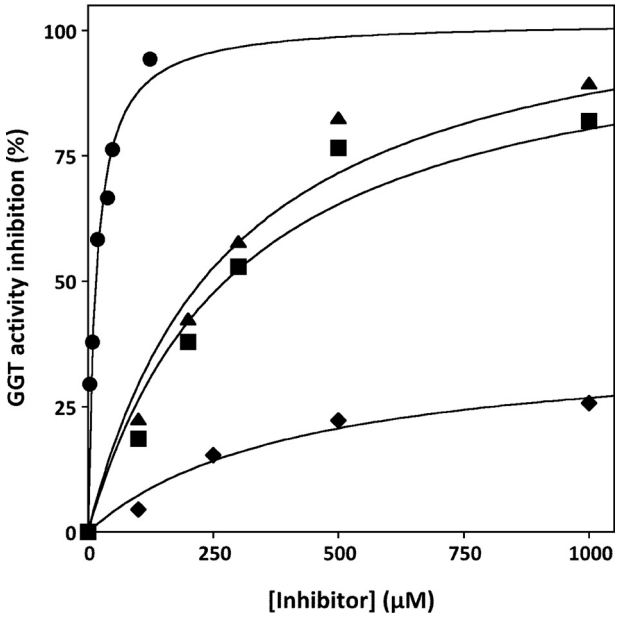

Figure 2. Inhibition of GGT activity. GGT activity was measured in the presence of 40 mM GlyGly and 3 mM GpNA at the indicated concentrations of ovo (●), erg (■), DON (▲), and DTT (♦) and is reported as percentage of the activity measured in the absence of the inhibitor (21 units). Data were fitted according to a rectangular hyperbolic binding function.

Results

Ovothiol inhibits GGT activity

Enzyme assays were carried out using both human GGT (hGGT) isolated from membranes of human liver cancer cell line HepG2 or chronic B leukemic cells HG3 cells and the commercial equine kidney GGT (eqGGT; with a high percentage of identity with hGGT), maintaining fixed and saturating concentrations of γ-glutamyl-*para*-nitroanilide (GpNa) and the acceptor glycyl-glycine (GlyGly) and varying the concentrations of the different testing compounds. Residual GGT activity in the presence of ovothiol A (ovo), isolated from *P. lividus* eggs in its disulfide form (41), was compared with that in the presence of the trimethyl-2-thiohistidine ergothioneine (erg) stabilized in thione form, the previously characterized GGT inhibitor DON (15), and dithiothreitol (DTT), used as a negative control (Fig. 2). Under these conditions, 50% GGT inhibition was obtained at 16 μM for ovo compared with 282 μM for DON, which was abandoned in clinical trials for toxicity (21), and with 297 μM for erg. Similar results were obtained with eqGGT in the presence of the different compounds. The addition of DTT did not induce any GGT-inhibitory action, thus excluding the possibility that the observed inhibitory effect was due to the intrinsic ability of an unspecific thiol to reduce cysteine or disulfides.

Kinetic analysis of GGT inhibition by ovothiol

To determine the mechanism of ovothiol-driven inhibition of GGT, kinetics of eqGGT activity were analyzed, in the absence or presence of the inhibitor, varying each of the substrates with the second maintained at a fixed concentration. In particular, when GlyGly (the acceptor substrate) concentration varied, GpNA was maintained at 3 mM; vice versa, GlyGly was maintained at 40 mM when GpNA concentration varied. The effect of different concentrations of ovo, DON, and erg on the

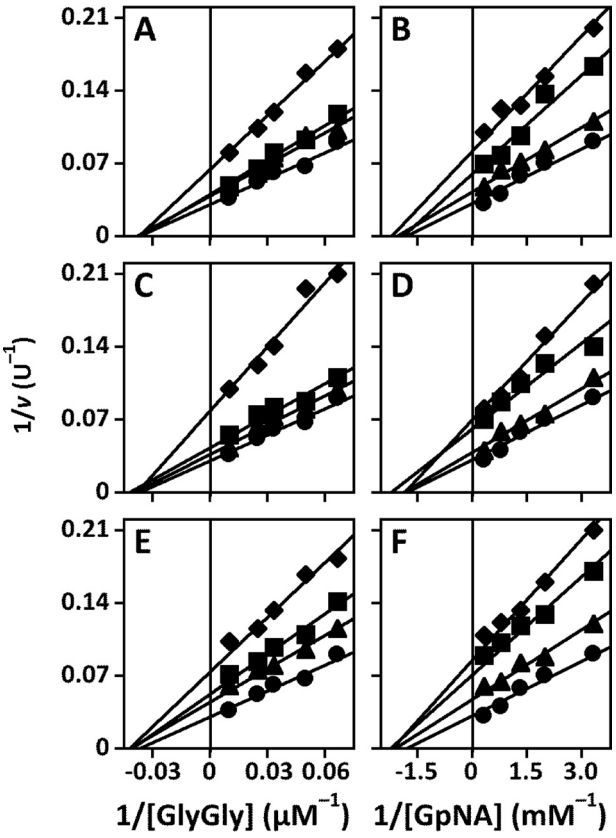

Figure 3. Kinetic analysis of GGT inhibition. EqGGT activity was assayed as reported under "Experimental procedures" in the presence of 3 mM GpNA and the indicated concentrations of GlyGly (*A*, *C*, and *E*) or in the presence of 40 mM GlyGly and the indicated concentrations of GpNA (*B*, *D*, and *F*). Double-reciprocal Lineweaver–Burk plots were obtained in the absence (●) or presence of 5 (▲), 10 (■), or 20 (◆) μM ovo (*A* and *B*) and 100 (▲), 200 (■), or 300 (◆) μM erg (*C* and *D*) and DON (*E* and *F*).

Table 1
Inhibition constants of GGT activity by sulfur-containing compounds
Data of apparent K_i were obtained as reported under "Experimental procedures" and are expressed as mean ± S.D. (n = 3).

Compound	Fixed substrate	Variable substrate	Apparent K_i (μM)
Ovo	GpNA	GlyGly	21 ± 7
DON	GpNA	GlyGly	141 ± 27
Erg	GpNA	GlyGly	171 ± 3
Ovo	GlyGly	GpNA	7 ± 1
DON	GlyGly	GpNA	83 ± 11
Erg	GlyGly	GpNA	111 ± 10

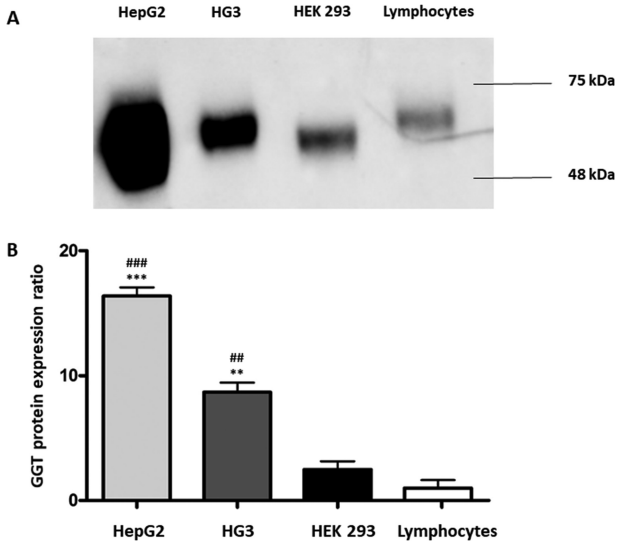

Figure 4. Protein expression analysis of hGGT. *A*, representative Western blot using hGGT-specific antibody against microsomal extracts of HG3 and HepG2 human cancer cells compared with normal lymphocytes and HEK 293 cells. *B*, protein expression levels were quantified by densitometric analysis using ImageJ software and normalized *versus* total protein content: **, p = 0.0048; ***, p = 0.0003 *versus* HEK 293 cells; ##, p = 0.0021; ###, p = 0.0002 *versus* lymphocytes. *Error bars* represent S.D. The significance was determined by Student's t test and post hoc analysis.

kinetics of eqGGT is shown in representative Lineweaver–Burk graphs reported in Fig. 3. The behavior of ovo inhibition (Fig. 3, *A* and *B*) accounted for a noncompetitive-like inhibition. In fact, the extrapolation of the fitting on the x axis approached very similar K_m values, whereas a decrease of V_{max} was observed in all cases. These data indicate that ovo has the same affinity for the free enzyme and the covalent E–γ-glutamyl complex, both when GpNA binds as donor substrate and GlyGly binds as acceptor. Similar kinetic behaviors with decreased V_{max} and roughly constant K_m values were also obtained in the presence of erg (Fig. 3, *C* and *D*) and DON (Fig. 3, *E* and *F*). The apparent K_i values obtained from nonlinear fitting in the Michaelis–Menten equation (Fig. S1) are reported in Table 1. The apparent K_i values obtained for each compound indicated that, among those tested, ovo is a more potent inhibitor compared with erg and DON, thus confirming the data reported in Fig. 2.

Ovothiol inhibits membrane-bound GGT of human cells

HepG2 and HG3 cells were tested for GGT expression and activity. Partially purified GGT extracts from two different biological samples containing the mature membrane-bound form of GGT were evaluated by immunoblotting using specific antibody against hGGT. Both cell lines showed a significant higher expression of the membrane-bound form of GGT (~64 kDa) compared with normal lymphocytes and human embryonic kidney (HEK) 293 cells (Fig. 4). Curiously, the molecular weight of GGT in HEK 293 was apparently lower compared with GGT from HepG2 and HG3, likely due to differences in the status of protein glycosylation. These results demonstrated that the tumoral cell lines investigated in this study expressed higher levels of GGT compared with nonmalignant cells.

To confirm that ovothiol inhibits membrane-bound GGT in dividing cells, we treated HG3 cells with 20 μM ovo and measured GGT activity and expression after 2 and 24 h. Ovo did not induce significant changes in GGT expression compared with non-treated cells at 2 h, except for a slight decrease of GGT expression at 24 h (Fig. 5, *A* and *B*). On the contrary, GGT activity normalized *versus* GGT content was significantly reduced both at 2 and 24 h (Fig. 5*C*). After 24 h, we also observed a significant increase of GSH levels in the cell medium, confirming the inhibition of its extracellular hydrolysis following GGT inhibition (Fig. 5*D*).

Ovothiol reduces cell proliferation in GGT-positive cell lines

To assess whether ovo was able to interfere with cell proliferation, HG3 and HepG2 cells were incubated in the presence of different concentrations of ovo, erg, and DON for 24–48 h. In the case of HG3 cells, the CyQuant assay, employed to measure proliferating cells, indicated a significant cytotoxic effect

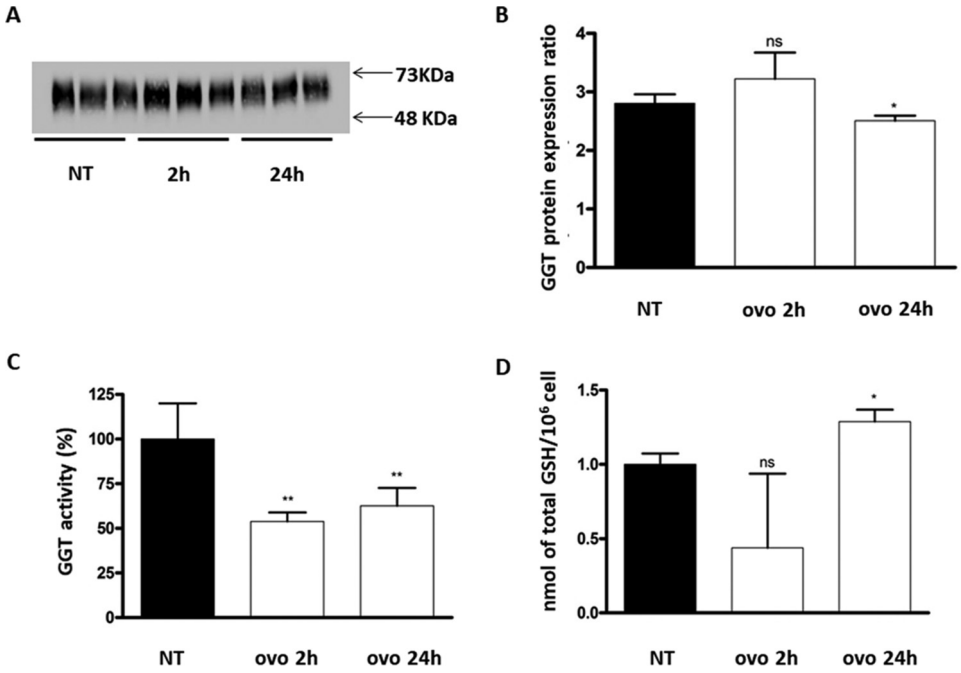

Figure 5. GGT activity and GSH content in HG3 upon treatment with ovothiol. *A*, representative Western blot performed with hGGT-specific antibody using microsomal extract of HG3 cells. *B*, protein expression levels analyzed by densitometric analysis and normalized to total protein content ($n = 3$). *, $p = 0.0403$ *versus* nontreated cells (*NT*). *C*, enzymatic activity of GGT evaluated on cell microsomal extracts containing membrane-bound GGT. The activity of GGT was normalized to the densitometric value of GGT protein band detected by immunoblotting ($n = 6$). **, $p = 0.0014$ (2 h); **, $p = 0.0075$ (24 h) *versus* nontreated cells. *D*, the levels of GSH were determined in the medium of cells. GSH content was normalized *versus* the number of cells ($n = 6$). *, $p = 0.0376$ *versus* nontreated cells. *Error bars* represent S.D. The significance was determined by the Student's *t* test and post hoc analysis. *ns*, not significant.

of 50 μM ovo at 24 h with a decrease in cell viability of about 80% (Fig. 6, *A* and *B*). Cells treated with erg were resistant to the treatment at both 24 and 48 h, also at the highest concentration (100 μM). In these conditions, we also observed increased cell proliferation. DON showed a significant reduction of cell viability (about 60–70%) at 48 h but less pronounced compared with ovo (Fig. 6*A*). Based on these results, we performed a dose-effect experiment applying a range of ovo concentrations between 5 and 100 μM. The resulting EC_{50} was about 29 μM. A similar trend was observed on HepG2 cells, which, in general, were more resistant to DON, erg, and ovo treatments (Fig. 6, *C* and *D*), although, similarly to HG3 cells, ovo was the most effective in reducing cell viability.

Ovothiol A induces autophagy in GGT-positive HG3 cell line

We previously demonstrated that ovo induced an autophagy-dependent form of cell death in HepG2 cells (41). Therefore, we verified whether a similar effect was detectable in the HG3 cell line. To this aim, cells were stained with Cyto-ID® autophagy dye, a fluorescent reagent able to be specifically incorporated into autophagosomes. Fluorescence staining indicated the presence of autophagic vacuoles in cells incubated with ovo and DON, with a maximum effect for the former in the range of 20–50 μM (Fig. 7). Erg did not induce any significant variation compared with untreated cells or cells treated with vehicle (data not shown). As positive controls, we treated HG3 cells for 24 h with 25 μM quercetin (Fig. 7*B*). The vacuoles stained by Cyto-ID were clearly visible under phase-contrast microscopy (Fig. 7*A*). The result of the Cyto-ID assay overlapped with the quantification obtained by measuring the fluorescence emitted by vacuoles (FITC) and by normalizing with that deriving from nuclei through a spectrofluorimetric reading (Fig. 7*B*). We were also able to confirm the modulation of autophagy by ovo and DON and, at a lesser extent, by erg in HepG2 cells (Fig. S2). The activation of an autophagic process was confirmed by the increased expression of microtubule-associated protein 1A/1B light chain 3 (LC3) bands after treatment for 24 h with ovo and DON (Fig. 7*C*). Densitometric analysis of the relevant bands indicated a 6-fold increase of the lipidated form (LC3-II), an essential factor for autophagosome formation (46).

Activation of a cytotoxic autophagy by ovothiol in HG3 cells

Data obtained from Cyto-ID assays and LC3-II expression confirmed the involvement of autophagy in killing HG3 cells after ovo treatment (Fig. 6). Therefore, we tried to characterize the type of autophagy activated by ovo among those associated with cancer cell growth (47). We could *bona fide* exclude cytostatic and cytoprotective autophagy, characterized by cell cycle arrest and cell survival, respectively. Therefore, we hypothesized the activation of a cytotoxic/nonprotective form of autophagy. To experimentally support this conclusion, we modulated autophagy flux using two different, widely employed pharmacological inhibitors, namely 3-methyladenine (MA) and bafilomycin (Baf-A1) (48, 49). In the presence of a "cytoprotective" autophagy, the inhibition of the autophagic flux by MA or Baf-A1 in combination with ovo should increase cell death. In contrast, the inhibition of nonprotective autophagy should not affect or rescue cells from ovo sensitivity. The latter hypothesis has been confirmed by the results reported in Fig. 8, where MA + ovo cotreatment or Baf-A1 + ovo cotreatment significantly rescued cell viability compared

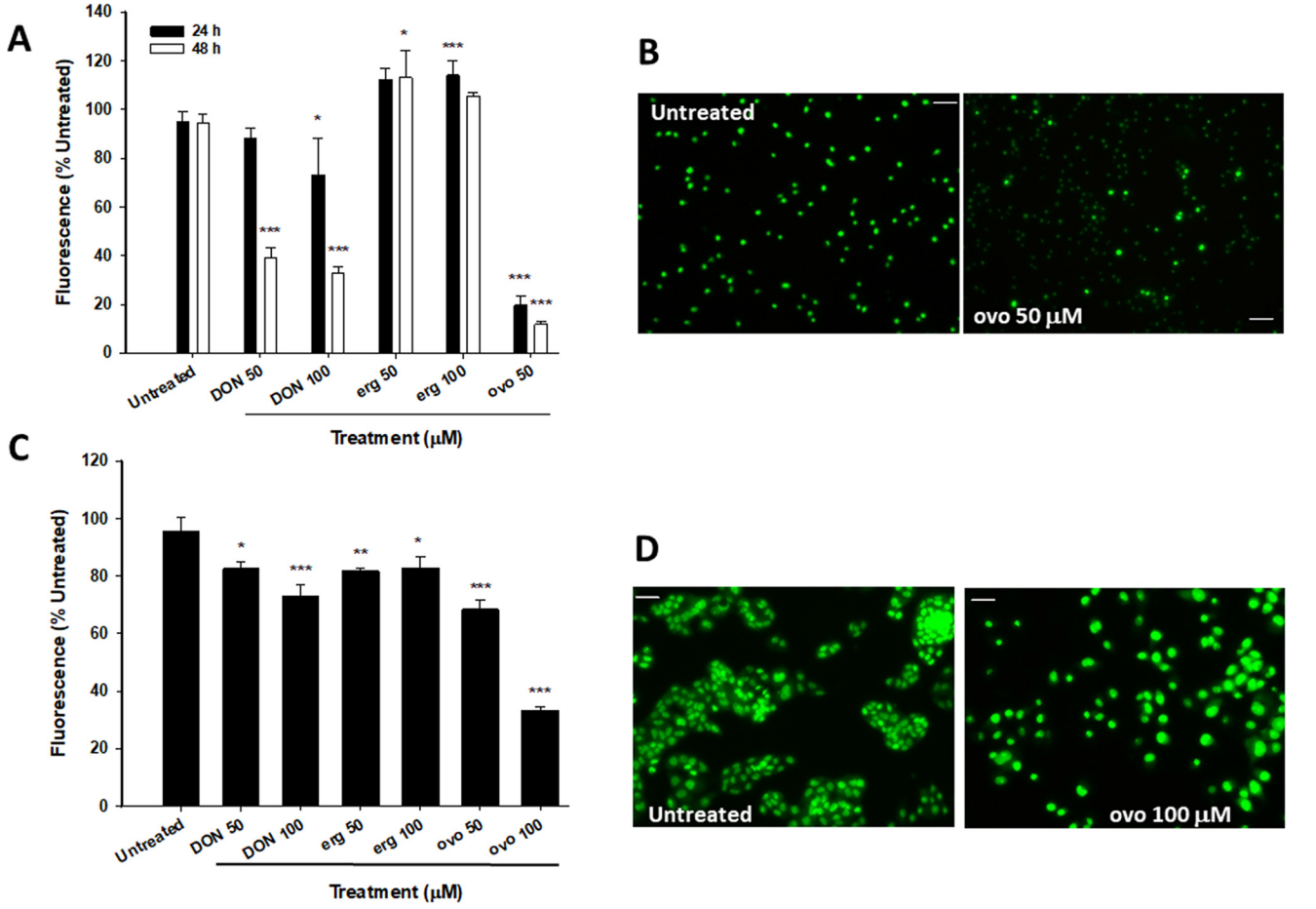

Figure 6. *A* and *C*, cell viability of HG3 (*A*) and HepG2 (*C*) cells treated with ovo (50–100 μM), DON (50–100 μM), and erg (50–100 μM). A CyQuant viability assay was performed after 24–48 h of treatment as indicated and described under "Experimental procedures." *Error bars* represent S.D. *Symbols* indicate significance: *, $p < 0.05$; **, $p < 0.01$; ***, $p < 0.001$ with respect to untreated cells. *B* and *D*, micrographs of HG3 (*B*) and HepG2 (*D*) cell nuclei stained with CyQuant fluorescent dye after 24 h of treatment with the indicated concentrations of ovo (Axiovert 200 microscope, FITC fluorescence filter, 200× *magnification*). *Scale bars*, 50 μm.

with the reduction induced by ovo treatment alone. Therefore, we concluded that ovo activates a nonprotective/cytotoxic form of autophagy in HG3 cells.

Activation of apoptotic cell death by ovothiol in HG3 cells

Following the demonstration that ovo induces a nonprotective form of autophagy, we investigated the possible origin of the massive cell death caused by this compound at 24 and 48 h (Fig. 6). Microscope observation of HG3 cells treated with ovo suggested the possible activation of apoptotic processes, as demonstrated by the presence and quantification of apoptotic nuclei (Fig. 9, *A* and *B*), which were confirmed by the 4-fold increase in caspase-3 activity (Fig. 9*C*), measured at an early time point (6 h). The rapid caspase cascade activation indicates that ovo specifically targets the apoptotic process, which does not represent an epiphenomenon due to the length of the treatment. It is worthwhile to note that both DON and erg did not produce any significant effect on caspase-3 activation but rather a decrease in caspase activity (Fig. 9*C*).

Ovothiol is not cytotoxic on nonmalignant cells

The most common inhibitors of GGT activity, for example DON and acivicin (36–38), show a high toxicity, limiting potential clinical applications. To test the cytotoxicity of ovo in nonmalignant cells, viability of HEK 293 was assessed after treatment for 24–48 h at concentrations of 20–100 μM. The results showed that ovo was not cytotoxic when compared with untreated cells but induced a slight increase in cell viability (Fig. 10).

Discussion

GGT plays a key role in maintaining cellular redox homeostasis, in detoxification processes, and in the evolution of many physiological disorders such as tumor progression, drug resistance, neurodegenerative diseases, the pathology of asthma, ischemia/reperfusion-induced renal injury, and liver fibrosis (7, 12–14). In particular, the high expression and/or activity of GGT in several human tumors can induce new protein synthesis and fast cell division (1, 6). For these reasons, inhibitors of GGT activity can sensitize GGT-positive tumors to chemotherapeutic treatment by limiting the supply of cysteine to tumor cells and blocking the accumulation of intracellular GSH. Acivicin, for example, has been used to deplete tumor GSH in combination with aggressive chemotherapy, resulting in complete cure of metastatic melanoma to the liver in 90% of test animals (50). However, most of the known GGT inhibitors are toxic or possess a limited efficacy for their potential use in clin-

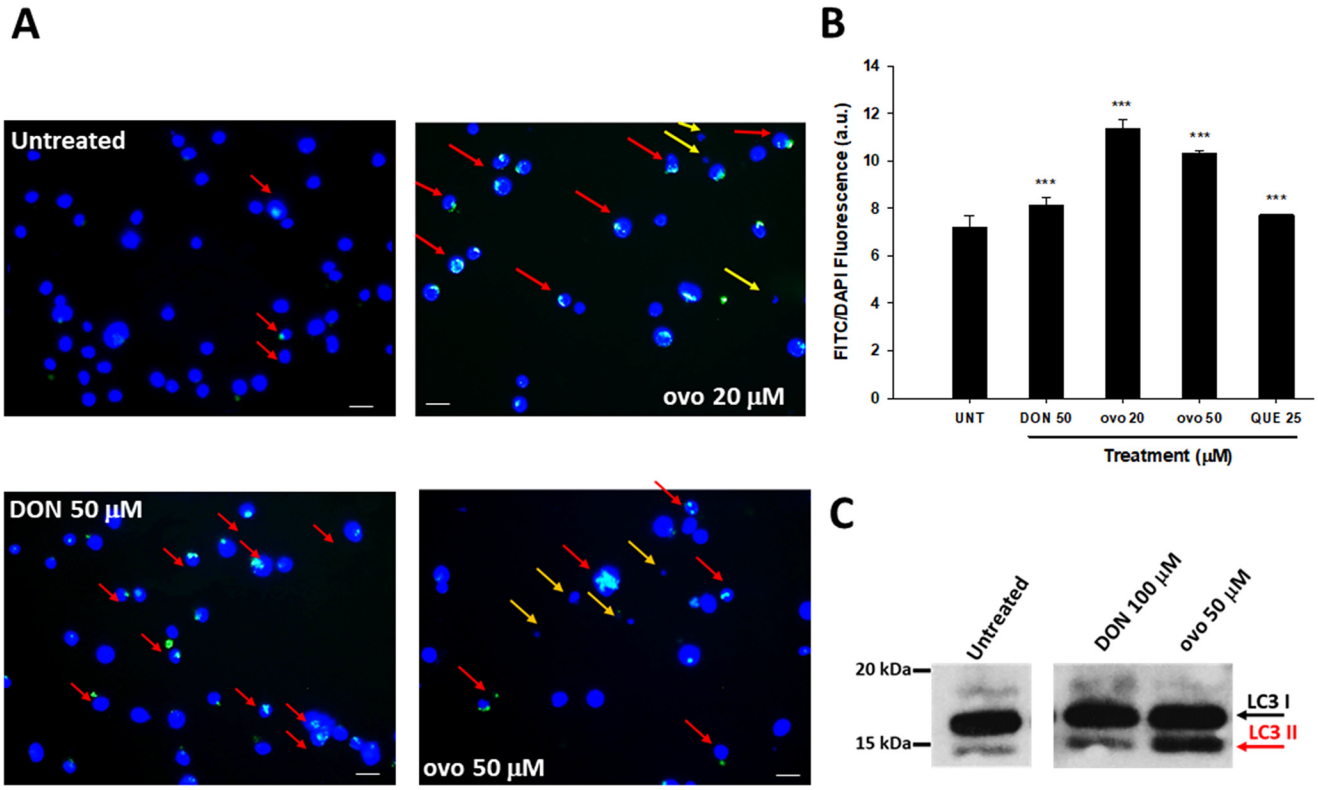

Figure 7. DON and ovo induce autophagy in HG3 cells. *A*, micrographs of autophagic vacuoles (*green*) and nuclei (*blue*) in untreated cells and after 24-h treatment with the indicated molecules. The photographs were taken with FITC and DAPI filters using a fluorescence invertoscope (Axiovert 200) with a total *magnification* of 400×. The Cyto-ID autophagy assay was performed as reported under "Experimental procedures." *Scale bars*, 20 μm. *B*, autophagosome quantification expressed as the FITC/DAPI fluorescence ratio in HG3 cells treated with different doses of ovo (20 and 50 μM) and DON (50 μM) using 25 μM quercetin as a positive control, respectively. The *bars* in the graphs indicate S.D.; *symbols* indicate significance: ***, $p < 0.001$ with respect to untreated cells. *C*, immunoblot of LC3-I and LC3-II expression in HG3 cells treated for 24 h with ovo (50 μM) and DON (100 μM), normalized for total protein content. Bands are representative of one of three separate experiments performed. *a.u.*, absorbance units.

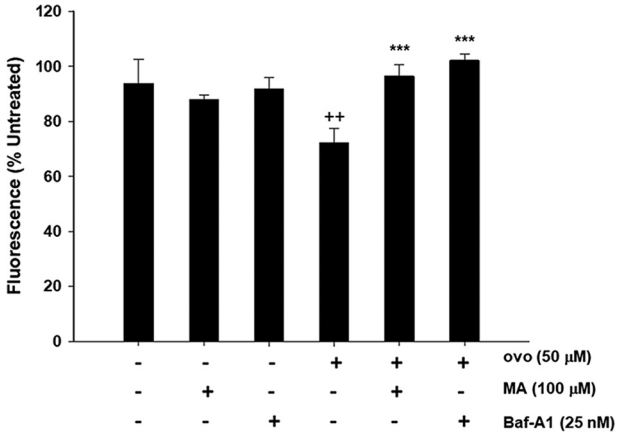

Figure 8. Activation of a nonprotective autophagy by ovo in HG3 cells. Cells were treated with ovo (50 μM) alone, autophagy inhibitor MA (100 μM) or Baf-A1 (25 nM), or their combination. The CyQuant viability assay was performed after 24 h of incubation as described. *Error bars* represent S.D.; *symbols* indicate significance: ++, $p < 0.01$ with respect to untreated cells; ***, $p < 0.001$ with respect to ovo-treated cells.

ics; therefore, the discovery of novel and less toxic GGT inhibitors already represents a challenge for physiological disorders associated with high levels of GGT (2).

In a previous study, we demonstrated that ovo purified from sea urchin eggs reduced cell proliferation through an autophagic mechanism in HepG2 cells (41). In that case, most of the ovo administered to the cells remained in the cell medium, thus prompting us to speculate that ovo could interact with a membrane surface protein complex. Among these, GGT represents one of the most expressed enzyme on the surface of liver cells.

In this study, we identified GGT as a direct target of ovo action, leading to the discovery of a novel class of GGT inhibitors, *i.e.* marine 5-thiohistidines. Kinetic studies on hGGT and eqGGT in the presence of these compounds pointed to a noncompetitive-like inhibition relative to the donor and the acceptor substrate. Although in a strictly noncompetitive inhibition identical values of K_i should be obtained regardless of the fixed substrate used in the kinetic assay, the complexity of the ping–pong mechanism might explain the slight differences of the inhibition constant for ovo, DON, and erg (see Table 1). In contrast to competitive inhibitors, which lose potency as substrate concentration rises, uncompetitive inhibitors become more potent as the substrate concentration rises in an inhibited open system (51). Therefore, ovo can result in a more advantageous effect compared with other competitive inhibitors mainly *in vivo* when GSH concentrations rise following GGT enzymatic inhibition. Structural properties of ovo increased inhibitory activity more than 10-fold compared with other inhibitors (*e.g.* DON) but without being accompanied by an increase in toxicity. In fact, the *in vitro* cytotoxicity profile of ovo is favorable because it does not induce cell death in HEK 293, at least up to 100 μM concentration. Curiously, ovo induced an increase of nonmalignant cell vitality at 24 h. This

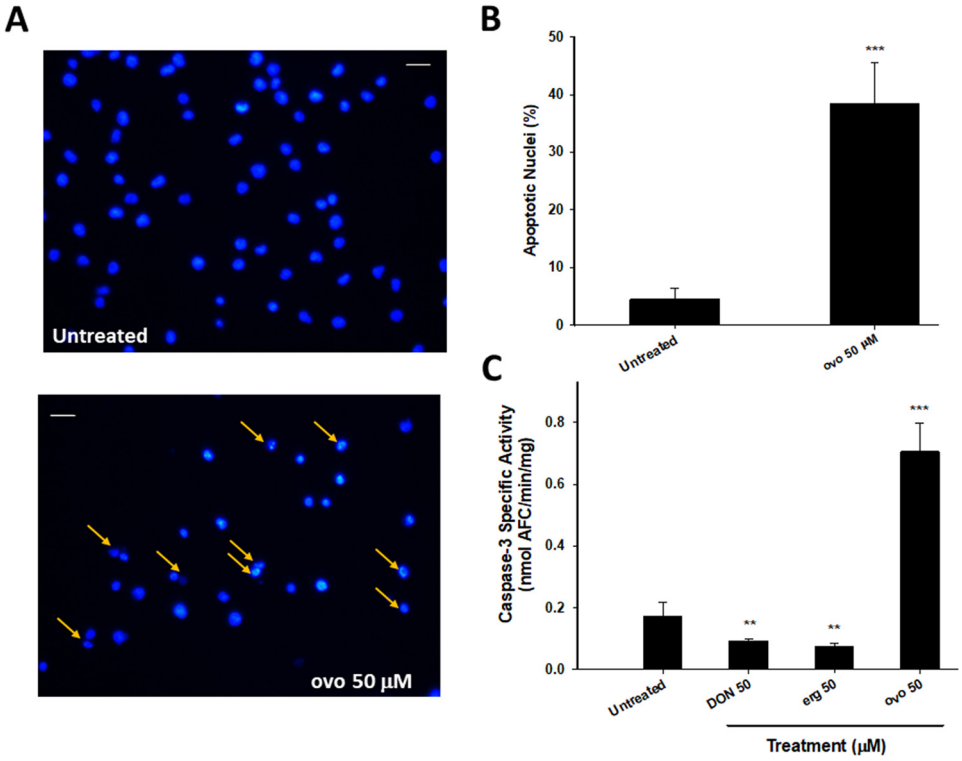

Figure 9. Ovo activates apoptosis in HG3 cells. *A* and *B*, cells were treated for 24 h with ovo (50 μM), and apoptotic nuclei, detected by Hoechst solution, were measured as percentage of total cells (>200/field). *Scale bars*, 20 μm. *C*, cells were treated for 6 h with ovo, DON, or erg at the indicated concentration, and caspase-3 specific activity was measured as described under "Experimental procedures." *Error bars* represent S.D.; *symbols* indicate significance: **, $p < 0.01$; ***, $p < 0.001$ with respect to untreated cells.

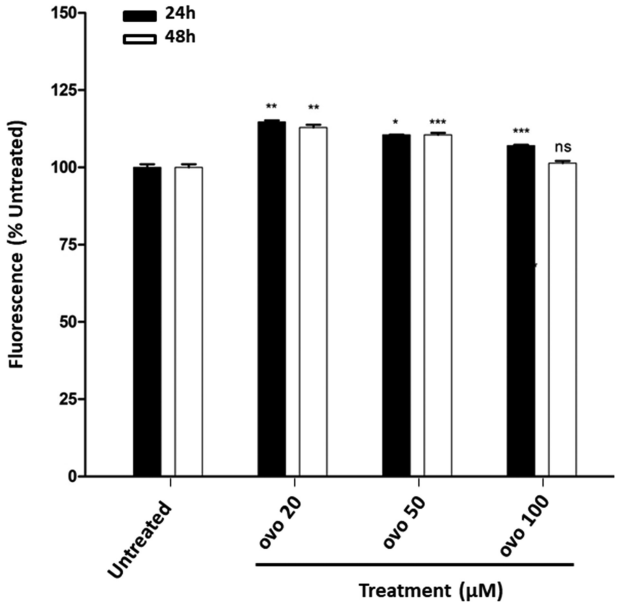

Figure 10. Cytotoxicity assay on HEK 293 cells. Cells were treated for 24 and 48 h with ovo at the indicated concentrations, and cell viability was measured by a resazurin-based assay ($n = 3$). *, $p = 0.0206$; **, $p = 0.0021$; ***, $p = 0.0002$ *versus* untreated (24 h), **, $p = 0.0050$; ***, $p = 0.0003$; *ns*, not significant, *versus* untreated (48 h). *Error bars* represent S.D. The significance was determined by Student's *t* test and post hoc analysis.

phenomenon may account for an adaptive response of the cell known as hormesis, which deserves further investigations. On the contrary, the trimethyl-2-thiohistidine erg appeared as a very weak inhibitor of GGT activity. This observation may suggest that the disulfide form of 5-thiohistidines has a strong effect in inhibiting GGT activity, likely due to a major steric hindrance or to the higher reactivity of the sulfhydryl group, compared with the stabilized thione form of erg.

Most importantly, ovo reduced cell proliferation in GGT-positive cell lines with concomitant occurrence of a nonprotective/cytotoxic form of autophagy, indicating that the inhibition of GGT activity is likely involved in the modulation of autophagic mechanisms. Indeed, our data demonstrated that both ovo and DON induced autophagy, with the former being more effective. This is in agreement with the lower IC_{50} showed by ovo *versus* DON as a result of the inhibition of GGT enzymatic activity (Fig. 2). The capacity of ovo to specifically activate nonprotective autophagy by modulating the autophagic flux has been confirmed by the increase in autophagosome formation and overexpression of the lipidated form of LC3 (LC3-II). Conversely, the more efficient GGT inhibition associated with ovo treatment compared with DON is supported by the observed induction of caspase-3 activation and the consequent formation of apoptotic nuclei. Several explanations can be provided to understand the dual role of ovo in inducing both apoptosis and nonprotective autophagy. It is well-known that these two processes are functionally and biochemically connected, with key factors (*e.g.* p53, death-associated protein kinase, Bcl-2 family members, and several oncogenes) affecting many signal transduction pathways regulating both autophagy and apoptosis (52). It is possible the GGT inhibition by ovo triggers one of these pathways, generating a sequential activation of both processes. Specifically, a rapid apoptotic induction after 6 h of ovo treatment (Fig. 9*C*) and a later (24 h) autophagy flux modula-

tion were measured in HG3 cells (Fig. 7, *A* and *B*). On the contrary, we detected only lethal autophagy in HepG2 cells treated with ovo as reported previously (41). A possible hypothesis is that the initial apoptotic induction in HG3 cells leads to caspase-dependent cleavage of autophagy-related (ATG) proteins necessary to induce a cytoprotective form of autophagy. This event blocks autophagic flux, resulting in cytotoxic autophagy at later stages (52). The autophagic switch from a protective process to cell death depends upon overcoming a resistance threshold, which differs in cancer cells of different origins, in relation to the stimulus applied. In other words, apoptotic induction followed by lethal autophagy may rely on the intracellular status of key regulators such as p53 or BH3-only factors, both involved in the switch between apoptosis and autophagy (52) However, we cannot exclude that the two events, autophagy and apoptosis, are parallel but due to independent molecular mechanisms, in accord with the pleiotropic nature of ovo. In fact, the inhibition of extracellular GSH hydrolysis is known to block cysteine uptake, which is responsible for maintaining the cellular reductive potential and preventing the apoptotic cascade (53). Therefore, a strong GGT inhibition favors the establishment of a cellular oxidative environment, which can, in turn, promote the apoptotic cascade. In addition, it is also possible to hypothesize the existence of two different populations of cancer cells, which, in relation to their cell cycle phase, can differently react to ovo treatment. Consequently, one population shows high sensitivity to the direct proapoptotic effects of ovo, whereas the other responds by activating nonprotective autophagy and triggering autophagic cell death. Future studies will be devoted to discriminating among these different hypotheses. Overall, the data presented here are in agreement with the presence of multiple routes activated by ovo to kill cancer cells via inhibition of GGT enzyme.

Moreover, ovo, exerting a more powerful inhibitory activity on GGT, also induced a stronger decrease of cell proliferation at lower micromolar concentrations compared with DON. According to this, the EC_{50} of about 29 μM for ovo cytotoxicity in HG3 is comparable with the apparent K_i determined for GGT in the presence of ovo (21 μM).

Our working hypothesis is that GGT inhibition should block the continuous metabolism of extracellular GSH and the fast recovery of intracellular cysteine, necessary for new protein synthesis and rapid division. Indeed, we showed that, shortly after inhibition of membrane-bound GGT activity by ovo, GSH accumulated outside the cells (Fig. 5). This event should block the recycling of amino acids like cysteine and glycine, leading to cell stress and consequent apoptosis and autophagy induction. To the best of our knowledge, this should be the first time that the modulation of GGT activity has been associated with autophagic processes. Reduced autophagic activity was already observed several years ago in hepatocytes isolated from carcinogen-treated rats, characterized by GGT-positive loci (54). These cells survived much better than normal hepatocytes in culture under conditions of amino acid deprivation, suggesting the activation of a protective form of autophagy. These observations suggested that the anabolic advantage of protective autophagy may possibly contribute to the selective outgrowth of preneoplastic cells during the earliest stage of liver carcinogenesis. In this regard, ovo-dependent GGT inhibition can selectively induce a nonprotective/cytotoxic autophagy in malignant cells compared with their normal counterpart where the autophagic mechanism remains finely regulated. Our findings confirm that GGT is overexpressed in malignant cell lines HepG2 and HG3 compared with normal cells (HEK 293 and lymphocytes) (Fig. 4) and that ovothiol reduces cell viability only for the former. This suggest that physiological levels of GGT in normal cells like hepatocytes may account for fine regulation of the cellular redox homeostasis, GSH levels, amino acid metabolism, and finally controlled autophagy. In contrast, GGT-overexpressing cell lines can be characterized by modulation of the autophagic mechanisms favoring cancer cell survival and proliferation. This is in agreement with the well-described and now consolidated dual and opposite role of autophagy in cancer (52).

In conclusion, because clinical application of known GGT inhibitors was abandoned due to their toxicity and/or low effectiveness, the development of more efficient and less toxic compounds such as the class of 5-thiohistidines holds great promise for improving cancer therapy of GGT-positive tumors and other GGT-dependent pathologies. In regard to this concern, we have recently demonstrated the efficacy of ovo to ameliorate liver fibrosis in an *in vivo* murine model (14). In addition, we demonstrated that mice affected by liver fibrosis exhibited higher membrane-bound GGT activity and that the administration of ovo induced the reduction of GGT activity. These results could help in the near future to develop new therapeutic approaches based on marine natural products.

Experimental procedures

Enzyme isolation and GGT activity assay

GGT was isolated from HepG2 and HG3 cell lines as described by King *et al.* (26). Cells were homogenized in 4 volumes of 25 mM Tris·Cl, pH 7.5, containing 0.33 M sucrose, 0.2 mM EDTA, 1 μM leupeptin, and 1.4 μg/ml aprotinin. A 9,000 $\times$ *g* supernatant was spun at 100,000 $\times$ *g* for 1 h. The microsomal pellet, resuspended in 25 mM Tris·Cl, pH 7.35, 0.5% Triton X-100, 1 μM leupeptin, 1.4 μg/ml aprotinin, was centrifuged again at 100,000 $\times$ *g* for 1 h. The supernatant was aliquoted, stored at −80 °C, and then assayed for GGT protein expression and activity. GGT activity was determined by a colorimetric test. The assay buffer contained 100 mM Tris·Cl, pH 7.8, or 1$\times$ PBS, pH 7.4. Each reaction contained 1 mM GpNA as a donor substrate and 40 mM GlyGly as an acceptor substrate. The formation of product, *p*-nitroaniline, was continuously monitored at room temperature at 405 nm using a Bio-Rad 680 microplate reader with Microplate Manager 5.2 (Bio-Rad) software. One unit of GGT activity was defined as the amount of GGT that released 1 μmol of *p*-nitroaniline/min at room temperature using 10000 $M^{-1}\cdot cm^{-1}$ as the molar absorption coefficient, derived as reported previously (55). All the substrates for GGT assay (GpNA, GlyGly, and eqGGT) and the compounds tested as inhibitors (erg, DON, and DTT) were purchased from Sigma-Aldrich.

Kinetic studies and data analysis

EqGGT was purchased from Sigma-Aldrich and used to carry out kinetics studies. The assay buffer contained 100 mM Na_2HPO_4, pH 7.4, with 3.2 mM KCl, 1.8 mM KH_2PO_4, and 27.5 mM NaCl. The concentrations of the substrate GpNA and the acceptor GlyGly were varied as indicated in the figure legends. Aliquots of 0.5–1 μl of GGT (1 mg/ml) were added to start the reaction, which was time-monitored as described above using a Cary100 spectrophotometer (Agilent). The initial velocity of the reaction was derived from the linear part of the kinetics. Data were nonlinear fitted to the Michaelis–Menten equation using Kaleidagraph™ 4.1 software (Synergy).

The apparent inhibition constant (K_i) were calculated using the following equation.

$$V_{max}' = V_{max}/(1 + [I]/K_i) \quad \text{(Eq. 1)}$$

in which V_{max} and V_{max}' represent the V_{max} in the absence or presence of [I], the concentration of the inhibitor. The apparent K_i values obtained at each inhibitor concentration were averaged to obtain a unique value of apparent K_i for each compound. Kinetic parameters and their corresponding standard errors were evaluated using a simple weighting method (Student's *t* test).

Immunoblotting

After treatments, cells (0.5×10^6) were resuspended in lysis buffer, and total protein lysates (20 μg) were loaded on a 4–12% precast gel (Novex Bis-Tris precast gel, 4–12%; Life Technologies) using MES buffer according to the manufacturer's protocol. Immunoblotting was performed following standard procedures using as primary antibody anti-LC3 (Cell Signaling Technology, Milano, Italy). Polyvinylidene difluoride membranes were finally incubated with horseradish peroxidase–linked secondary antibody against mouse or rabbit (GE Healthcare), and immunoblots were developed using the ECL Plus Western blotting Detection System kit (GE Healthcare). Band intensities were quantified by measuring their optical density on a Gel Doc 2000 apparatus (Bio-Rad) using Multi-Analyst software (Bio-Rad).

For GGT detection, microsomal extracts (5 μg) were run on a 12% SDS-polyacrylamide gel according to Laemmli (59). Following electrophoresis, proteins were transferred onto a polyvinylidene difluoride membrane (Millipore) using a Bio-Rad Trans-Blot apparatus and detected using a mouse anti-mouse anti-GGT mAb (Santa Cruz Biotechnology). The primary antibody was incubated at 4 °C overnight. The appropriate secondary antibody was added, and immunoreactive proteins were detected using enhanced chemiluminescence (Western-Bright™ ECL detection kit, Advansta) according to the manufacturer's instructions. Protein expression levels were analyzed by means of densitometric analysis using ImageJ software and normalized with respect to total protein content determined by Bradford (60) assay and checked by Coomassie Blue gel staining.

GSH assay

Total GSH levels were determined using a GSH Assay kit (Sigma). Briefly, cell culture media were added with 3 volumes of 5% 5-sulfosalicylic acid and mixed. Subsequently, 7 volumes of 5% 5-sulfosalicylic acid were added, mixed, incubated for 5 min at 4 °C, and finally centrifuged at 10,000 × *g* for 10 min. Diluted samples of the supernatants were used for the assay procedure where, following incubation with GSH reductase and NADPH, GSH was totally recovered in the reduced form, and its concentration was determined by monitoring the reduction of 5,5-dithiobis(2-nitrobenzoic acid) to 5-thio-2-nitrobenzoic spectrophotometrically (at 412 nm using a Thermo Scientific™ Multiskan™ FC microplate photometer).

Cell culture and viability assay

The HepG2 cell line, derived from a human hepatocellular carcinoma, and HG3 cell line, derived from chronic B-cell leukemia, were maintained in Dulbecco's modified Eagle's medium supplemented with 10% fetal bovine serum (Lonza, Belgium), 1% L-glutamine, 1% penicillin, and 1% streptomycin (Life Technologies) at 37 °C in a 5% CO_2 humidified atmosphere and harvested at ~90% confluence. For viability experiments, cells were plated in a 96-multiwell plate at a density of 2×10^4/well in a total volume of 0.1 ml. Subsequently, cells were treated for 24 h with ovo, erg, and DON at the indicated concentrations. Cell viability was determined by the CyQuant assay according to the manufacturer's instructions (Life Technologies). Fluorescence was measured at the excitation wavelength of 485 nm and 530-nm emission, and the results were expressed as percentage of fluorescence of the untreated control using a microplate reader (Synergy HT, BioTek, Milan, Italy). Experiments were performed in quadruplicate and repeated three times. Cells were photographed using a FITC filter (magnification, 400×) by an inverted microscope (Axiovert 200, Zeiss, Jena, Germany).

Peripheral blood samples were provided by anonymous healthy donors with informed consent. Lymphocytes were isolated following density gradient centrifugation (Ficoll-Paque Plus, GE Healthcare). Cells were washed three times in PBS, counted with trypan blue dye to assess their viability (cell viability >95%), and immediately cultured in RPMI 1640 medium supplemented with 1% penicillin/streptomycin, 2 mM L-glutamine, and 10% heat-inactivated autologous serum at 37 °C in a humidified atmosphere containing 5% CO_2.

Measurement of autophagy

Autophagy was monitored using the Cyto-ID Autophagy Detection kit (ENZO Life Science, Milan, Italy) as described (56, 57) using quercetin as the positive control. After incubation with ovo (20–100 μM), HepG2 or HG3 cells (2×10^4) were washed and incubated with the autophagy detection marker (Cyto-ID) and nuclear dye (Hoechst 33342). Cells were then rinsed with the assay buffer and photographed using a fluorescence microscope (Axiovert 200). Finally, autophagosomes were quantified by normalizing green (Cyto-ID) and blue (Hoechst) fluorescence using a microplate fluorescence reader (Synergy HT). Experiments were performed twice in quadruplicate.

Caspase-3 assay and apoptotic nuclei staining

To measure caspase-3 enzymatic activity, cells (1.0×10^6/ml) were incubated with the indicated compounds for 6 h and then lysed in lysis buffer (10 mM Hepes, pH 7.4, 2 mM EDTA, 0.1% CHAPS, 5 mM DTT, 1 mM phenylmethylsulfonyl fluoride, 10 μg/ml pepstatin-A, 10 μg/ml aprotinin, 20 μg/ml leupeptin). Cell extracts (10 μg) were mixed with caspase-3 reaction buffer and the conjugated amino-4-trifluoromethylcoumarin (AFC) substrates benzyloxycarbonyl-Asp (OMe)-Glu (OMe)-Val-Asp (OMe)-AFC (Z-DEVD-AFC). The samples were incubated at 37 °C for 30 min. Upon proteolytic cleavage of the substrates by caspase-3, the free fluorochrome AFC was detected by a spectrofluorometer multiplate reader (Bio-Tek Instruments) with excitation at 400 ± 20 nm and emission at 530 ± 20 nm. To quantify enzymatic activities, an AFC standard curve was determined. Caspase-3 specific activity was calculated as nmol of AFC produced/min/μg of proteins at 37 °C in the presence of saturating substrate concentrations (50 μM) (58).

For apoptotic nuclei staining after incubation with ovothiol A, cells were collected and centrifuged at 400 × *g* for 5 min, washed in PBS, and stained at 37 °C with Hoechst solution (33268, ENZO Life Science) dissolved in PBS (5 μg/ml) for 30 min. Cells were washed in PBS, and apoptotic nuclei were photographed and counted using a fluorescence microscope (>100 cells/field, 400× magnification).

Cytotoxicity assays

For cytotoxicity assays, HEK 293 cells were plated in 384-multiwell plates (2×10^3 cell/well) and treated with ovo, erg, and DON at the indicated concentrations for 24–48 h. Cytotoxicity was assessed by resazurin-based assays (CellTiter-Blue® Cell Viability Assay, Promega) according to the manufacturer's recommendations using a Spark® multimode microplate reader (TECAN). Experiments were performed in triplicate. Data were expressed as fluorescence $560/590_{nm}$.

Statistical analysis

As appropriate, comparisons among groups were made by Student's *t* test or analysis of variance followed by a Bonferroni or Tukey's multiple comparison test. Values of $p < 0.05$ were considered as significant.

Author contributions—M. B., M. R., M. M., A. P., G. L. R., and I. C. data curation; M. B., M. R., M. M., A. P., G. L. R., and I. C. formal analysis; M. B., A. P., G. L. R., and I. C. validation; M. B., M. R., M. M., A. P., G. L. R., and I. C. investigation; M. B., M. R., M. M., A. P., G. L. R., and I. C. methodology; M. B., M. R., M. M., A. P., G. L. R., and I. C. writing-review and editing; M. M., A. P., G. L. R., and I. C. conceptualization; A. P., G. L. R., and I. C. funding acquisition; G. L. R. and I. C. supervision; I. C. writing-original draft.

Acknowledgments—We thank Davide Caramiello and the service Marine Resources for sea urchin maintenance and gamete collection. We thank Prof. Alessio Peracchi for helpful discussion on enzyme inhibition.

References

1. Hanigan, M. H. (2014) γ-Glutamyl transpeptidase: redox regulation and drug resistance. *Adv. Cancer Res.* **122,** 103–141 CrossRef Medline
2. Castellano, I., and Merlino, A. (2012) γ-Glutamyltranspeptidases: sequence, structure, biochemical properties, and biotechnological applications. *Cell. Mol. Life Sci.* **69,** 3381–3394 CrossRef Medline
3. Castellano, I., and Merlino, A. (2013) *γ-Glutamyl Transpeptidases: Structure and Function*, Springer, Basel, Switzerland
4. Hanigan, M. H., Gallagher, B. C., Townsend, D. M., and Gabarra, V. (1999) γ-Glutamyl transpeptidase accelerates tumor growth and increases the resistance of tumors to cisplatin *in vivo*. *Carcinogenesis* **20,** 553–559 CrossRef Medline
5. Hanigan, M. H., Frierson, H. F. Jr, Swanson, P. E., and De Young, B. R. (1999) Altered expression of γ-glutamyl transpeptidase in human tumors. *Hum. Pathol.* **30,** 300–305 CrossRef Medline
6. Pompella, A., De Tata, V., Paolicchi, A., and Zunino, F. (2006) Expression of γ-glutamyltransferase in cancer cells and its significance in drug resistance. *Biochem. Pharmacol.* **71,** 231–238 CrossRef Medline
7. Corti, A., Franzini, M., Paolicchi, A., and Pompella, A. (2010) γ-Glutamyltransferase of cancer cells at the crossroads of tumor progression, drug resistance and drug targeting. *Anticancer Res.* **30,** 1169–1181 Medline
8. Benlloch, M., Ortega, A., Ferrer, P., Segarra, R., Obrador, E., Asensi, M., Carretero, J., and Estrela, J. M. (2005) Acceleration of glutathione efflux and inhibition of γ-glutamyltranspeptidase sensitize metastatic B16 melanoma cells to endothelium-induced cytotoxicity. *J. Biol. Chem.* **280,** 6950–6959 CrossRef Medline
9. Benlloch, M., Mena, S., Ferrer, P., Obrador, E., Asensi, M., Pellicer, J. A., Carretero, J., Ortega, A., and Estrela, J. M. (2006) Bcl-2 and Mn-SOD antisense oligodeoxynucleotides and a glutamine-enriched diet facilitate elimination of highly resistant B16 melanoma cells by tumor necrosis factor-α and chemotherapy. *J. Biol. Chem.* **281,** 69–79 CrossRef Medline
10. Ruoso, P., and Hedley, D. W. (2004) Inhibition of γ-glutamyl transpeptidase activity decreases intracellular cysteine levels in cervical carcinoma. *Cancer Chemother. Pharmacol.* **54,** 49–56 CrossRef Medline
11. Lieberman, M. W., Wiseman, A. L., Shi, Z. Z., Carter, B. Z., Barrios, R., Ou, C. N., Chévez-Barrios, P., Wang, Y., Habib, G. M., Goodman, J. C., Huang, S. L., Lebovitz, R. M., and Matzuk, M. M. (1996) Growth retardation and cysteine deficiency in γ-glutamyl transpeptidase-deficient mice. *Proc. Natl. Acad. Sci. U.S.A.* **93,** 7923–7926 CrossRef Medline
12. Yamamoto, S., Watanabe, B., Hiratake, J., Tanaka, R., Ohkita, M., and Matsumura, Y. (2011) Preventive effect of GGsTop, a novel and selective γ-glutamyl transpeptidase inhibitor, on ischemia/reperfusion-induced renal injury in rats. *J. Pharmacol. Exp. Ther.* **339,** 945–951 CrossRef Medline
13. Tuzova, M., Jean, J. C., Hughey, R. P., Brown, L. A., Cruikshank, W. W., Hiratake, J., and Joyce-Brady, M. (2014) Inhibiting lung lining fluid glutathione metabolism with GGsTop as a novel treatment for asthma. *Front. Pharmacol.* **5,** 179 CrossRef Medline
14. Brancaccio, M., D'Argenio, G., Lembo, V., Palumbo, A., and Castellano, I. (2018) Antifibrotic effect of marine ovothiol in an *in vivo* model of liver fibrosis. *Oxid. Med. Cell. Longev.* **2018,** 5045734 CrossRef Medline
15. Terzyan, S. S., Cook, P. F., Heroux, A., and Hanigan, M. H. (2017) Structure of 6-diazo-5-oxo-norleucine-bound human γ-glutamyl transpeptidase 1, a novel mechanism of inactivation. *Protein Sci.* **26,** 1196–1205 CrossRef Medline
16. Tate, S. S., and Meister, A. (1978) Serine-borate complex as a transition-state inhibitor of γ-glutamyl transpeptidase. *Proc. Natl. Acad. Sci. U.S.A.* **75,** 4806–4809 CrossRef Medline
17. Lherbet, C., and Keillor, J. W. (2004) Probing the stereochemistry of the active site of γ-glutamyl transpeptidase using sulfur derivatives of L-glutamic acid. *Org. Biomol. Chem.* **2,** 238–245 CrossRef Medline
18. Han, L., Hiratake, J., Tachi, N., Suzuki, H., Kumagai, H., and Sakata, K. (2006) γ-(Monophenyl) phosphono glutamate analogues as mechanism-based inhibitors of γ-glutamyl transpeptidase. *Bioorg. Med. Chem.* **14,** 6043–6054 CrossRef Medline

19. Han, L., Hiratake, J., Kamiyama, A., and Sakata, K. (2007) Design, synthesis, and evaluation of γ-phosphono diester analogues of glutamate as highly potent inhibitors and active site probes of γ-glutamyl transpeptidase. *Biochemistry* **46,** 1432–1447 CrossRef Medline
20. Ahluwalia, G. S., Grem, J. L., Hao, Z., and Cooney, D. A. (1990) Metabolism and action of amino acid analog anti-cancer agents. *Pharmacol. Ther.* **46,** 243–271 CrossRef Medline
21. Lyons, S. D., Sant, M. E., and Christopherson, R. I. (1990) Cytotoxic mechanisms of glutamine antagonists in mouse L1210 leukemia. *J. Biol. Chem.* **265,** 11377–11381 Medline
22. Taylor, S. A., Crowley, J., Pollock, T. W., Eyre, H. J., Jaeckle, C., Hynes, H. E., and Stephens, R. L. (1991) Objective antitumor activity of acivicin in patients with recurrent CNS malignancies: a Southwest Oncology Group trial. *J. Clin. Oncol.* **9,** 1476–1479 CrossRef Medline
23. Kamiyama, A., Nakajima, M., Han, L., Wada, K., Mizutani, M., Tabuchi, Y., Kojima-Yuasa, A., Matsui-Yuasa, I., Suzuki, H., Fukuyama, K., Watanabe, B., and Hiratake, J. (2016) Phosphonate-based irreversible inhibitors of human γ-glutamyl transpeptidase (GGT). GGsTop is a non-toxic and highly selective inhibitor with critical electrostatic interaction with an active-site residue Lys562 for enhanced inhibitory activity. *Bioorg. Med. Chem.* **24,** 5340–5352 CrossRef Medline
24. Shimamura, Y., Takeuchi, I., Terada, H., and Makino, K. (2019) Therapeutic effect of GGsTop, selective γ-glutamyl transpeptidase inhibitor, on a mouse model of 5-fluorouracil-induced oral mucositis. *Anticancer Res.* **39,** 201–206 CrossRef Medline
25. Terzyan, S. S., Burgett, A. W., Heroux, A., Smith, C. A., Mooers, B. H., and Hanigan, M. H. (2015) Human γ-glutamyl transpeptidase 1: structures of the free enzyme, inhibitor-bound tetrahedral transition states, and glutamate-bound enzyme reveal novel movement within the active site during catalysis. *J. Biol. Chem.* **290,** 17576–17586 CrossRef Medline
26. King, J. B., West, M. B., Cook, P. F., and Hanigan, M. H. (2009) A novel, species-specific class of uncompetitive inhibitors of γ-glutamyl transpeptidase. *J. Biol. Chem.* **284,** 9059–9065 CrossRef Medline
27. Jacob, C. (2006) A scent of therapy: pharmacological implications of natural products containing redox-active sulfur atoms. *Nat. Prod. Rep.* **23,** 851–863 CrossRef Medline
28. Seebeck, F. P. (2013) Thiohistidine biosynthesis. *Chimia* **67,** 333–336 CrossRef Medline
29. Castellano, I., and Seebeck, F. P. (2018) On ovothiol biosynthesis and biological roles: from life in the ocean to therapeutic potential. *Nat. Prod. Rep.* **35,** 1241–1250 CrossRef Medline
30. Palumbo, A., Castellano, I., and Napolitano, A. (2018) Ovothiol: a potent natural antioxidant from marine organisms, in *Blue Biotechnology: Production and Use of Marine Molecules* (Barre, S., and Bates, S. S., eds) pp. 583–610, Wiley VCH, Weinheim, Germany
31. Holler, T. P., and Hopkins, P. B. (1988) Ovothiols as biological antioxidants. The thiol groups of ovothiol and glutathione are chemically distinct. *J. Am. Chem. Soc.* **110,** 4837–4838 CrossRef
32. Turner, E., Hager, L. J., and Shapiro, B. M. (1988) Ovothiol replaces glutathione peroxidase as a hydrogen peroxide scavenger in sea urchin eggs. *Science* **242,** 939–941 CrossRef Medline
33. Shapiro, B. M. (1991) The control of oxidant stress at fertilization. *Science* **252,** 533–536 CrossRef Medline
34. Spies, H. S., and Steenkamp, D. J. (1994) Thiols of intracellular pathogens. Identification of ovothiol A in *Leishmania donovani* and structural analysis of a novel thiol from *Mycobacterium bovis*. *Eur. J. Biochem.* **224,** 203–213 CrossRef Medline
35. Rohl, I., Schneider, B., Schmidt, B., and Zeeck, E. (1999) L-Ovothiol A: the egg release pheromone of the marine polychaete *Platynereis dumerilii*: Annelida: Polychaeta. *Z. Naturforsch. C* **54,** 1145–1147 CrossRef
36. Selman-Reimer, S., Duhe, R. J., Stockman, B. J., and Selman, B. R. (1991) L-1-*N*-Methyl-4-mercaptohistidine disulfide, a potential endogenous regulator in the redox control of chloroplast coupling factor-I in *Dunaliella*. *J. Biol. Chem.* **266,** 182–188 Medline
37. O'Neill, E. C., Trick, M., Hill, L., Rejzek, M., Dusi, R. G., Hamilton, C. J., Zimba, P. V., Henrissat, B., and Field, R. A. (2015) The transcriptome of *Euglena gracilis* reveals unexpected metabolic capabilities for carbohydrate and natural product biochemistry. *Mol. Biosyst.* **11,** 2808–2820 CrossRef Medline
38. Braunshausen, A., and Seebeck, F. P. (2011) Identification and characterization of the first ovothiol biosynthetic enzyme. *J. Am. Chem. Soc.* **133,** 1757–1759 CrossRef Medline
39. Naowarojna, N., Huang, P., Cai, Y., Song, H., Wu, L., Cheng, R., Li, Y., Wang, S., Lyu, H., Zhang, L., Zhou, J., and Liu, P. (2018) *In vitro* reconstitution of the remaining steps in ovothiol A biosynthesis: C-S lyase and methyltransferase reactions. *Org. Lett.* **20,** 5427–5430 CrossRef Medline
40. Castellano, I., Migliaccio, O., D'Aniello, S., Merlino, A., Napolitano, A., and Palumbo, A. (2016) Shedding light on ovothiol biosynthesis in marine metazoans. *Sci. Rep.* **6,** 21506 CrossRef Medline
41. Russo, G. L., Russo, M., Castellano, I., Napolitano, A., and Palumbo, A. (2014) Ovothiol isolated from sea urchin oocytes induces autophagy in the Hep-G2 cell line. *Mar. Drugs* **12,** 4069–4085 CrossRef Medline
42. Castellano, I., Di Tomo, P., Di Pietro, N., Mandatori, D., Pipino, C., Formoso, G., Napolitano, A., Palumbo, A., and Pandolfi, A. (2018) Anti-inflammatory activity of marine ovothiol A in an *in vitro* model of endothelial dysfunction induced by hyperglycemia. *Oxid. Med. Cell. Longev.* **2018,** 2087373 CrossRef Medline
43. Holler, T. P., Spaltenstein, A., Hopkins, P. B., Turner, E., Klevit, R. E., and Shapiro, B. M. (1987) Synthesis and structure reassignment of mercaptohistidines of marine origin. Syntheses of L-ovothiols A and C. *J. Org. Chem.* **52,** 4420–4421 CrossRef
44. Holler, T. P., Ruan, F., Spaltenstein, A., and Hopkins, P. B. (1989) Total synthesis of marine mercaptohistidines: ovothiols A, B, and C. *J. Org. Chem.* **54,** 4570–4575 CrossRef
45. Daunay, S., Lebel, R., Farescour, L., Yadan, J. C., and Erdelmeier, I. (2016) Short protecting-group-free synthesis of 5-acetylsulfanyl-histidines in water: novel precursors of 5-sulfanyl-histidine and its analogues. *Org. Biomol. Chem.* **14,** 10473–10480 CrossRef Medline
46. Klionsky, D. J., Abdelmohsen, K., Abe, A., Abedin, M. J., Abeliovich, H., Acevedo Arozena, A., Adachi, H., Adams, C. M., Adams, P. D., Adeli, K., Adhihetty, P. J., Adler, S. G., Agam, G., Agarwal, R., Aghi, M. K., *et al.* (2016) Guidelines for the use and interpretation of assays for monitoring autophagy (3rd edition). *Autophagy* **12,** 1–222 CrossRef Medline
47. Gewirtz, D. A. (2014) The four faces of autophagy: implications for cancer therapy. *Cancer Res.* **74,** 647–651 CrossRef Medline
48. Gewirtz, D. A. (2016) The challenge of developing autophagy inhibition as a therapeutic strategy. *Cancer Res.* **76,** 5610–5614 CrossRef Medline
49. Rubinsztein, D. C., Codogno, P., and Levine, B. (2012) Autophagy modulation as a potential therapeutic target for diverse diseases. *Nat. Rev. Drug Discov.* **11,** 709–730 CrossRef Medline
50. Mena, S., Benlloch, M., Ortega, A., Carretero, J., Obrador, E., Asensi, M., Petschen, I., Brown, B. D., and Estrela, J. M. (2007) Bcl-2 and glutathione depletion sensitizes B16 melanoma to combination therapy and eliminates metastatic disease. *Clin. Cancer Res.* **13,** 2658–2666 CrossRef Medline
51. Westley, A. M., and Westley, J. (1996) Enzyme inhibition in open systems. Superiority of uncompetitive agents. *J. Biol. Chem.* **271,** 5347–5352 CrossRef Medline
52. Mariño, G., Niso-Santano, M., Baehrecke, E. H., and Kroemer, G. (2014) Self-consumption: the interplay of autophagy and apoptosis. *Nat. Rev. Mol. Cell Biol.* **15,** 81–94 CrossRef Medline
53. Corti, A., Duarte, T. L., Giommarelli, C., De Tata, V., Paolicchi, A., Jones, G. D., and Pompella, A. (2009) Membrane γ-glutamyl transferase activity promotes iron-dependent oxidative DNA damage in melanoma cells. *Mutat. Res.* **669,** 112–121 CrossRef Medline
54. Schwarze, P. E., and Seglen, P. O. (1985) Reduced autophagic activity, improved protein balance and enhanced *in vitro* survival of hepatocytes isolated from carcinogen-treated rats. *Exp. Cell Res.* **157,** 15–28 CrossRef Medline
55. Lottenberg, R., and Jackson, C. M. (1983) Solution composition dependent variation in extinction coefficients for *p*-nitroaniline. *Biochim. Biophys. Acta* **742,** 558–564 CrossRef Medline

56. Tedesco, I., Russo, M., Bilotto, S., Spagnuolo, C., Scognamiglio, A., Palumbo, R., Nappo, A., Iacomino, G., Moio, L., and Russo, G. L. (2013) Dealcoholated red wine induces autophagic and apoptotic cell death in an osteosarcoma cell line. *Food Chem. Toxicol.* **60,** 377–384 CrossRef Medline
57. Russo, M., Milito, A., Spagnuolo, C., Carbone, V., Rosén, A., Minasi, P., Lauria, F., and Russo, G. L. (2017) CK2 and PI3K are direct molecular targets of quercetin in chronic lymphocytic leukaemia. *Oncotarget* **8,** 42571–42587 CrossRef Medline
58. Crowley, L. C., Marfell, B. J., and Waterhouse, N. J. (2016) Analyzing cell death by nuclear staining with Hoechst 33342. *Cold Spring Harb. Protoc.* **9,** 778–781 CrossRef Medline
59. Laemmli, U. K. (1970) Cleavage of structural proteins during the assembly of the head of bacteriophage T4. *Nature* **227**, 680–685 CrossRef Medline
60. Bradford, M. M. (1976) A rapid and sensitive method for the quantitation of microgram quantities of protein utilizing the principle of protein-dye binding. *Anal. Biochem.* **72,** 248–254 CrossRef Medline

Sulfur-containing histidine compounds inhibit γ-glutamyl transpeptidase activity in human cancer cells

Mariarita Brancaccio, Maria Russo, Mariorosario Masullo, Anna Palumbo, Gian Luigi Russo and Immacolata Castellano

J. Biol. Chem. 2019, 294:14603-14614.
doi: 10.1074/jbc.RA119.009304 originally published online August 2, 2019